Structural Engineering and Mechanics, *Vol. 65, No. 2 (2018) 141-154*
DOI: https://doi.org/10.12989/sem.2018.65.2.141

Numerical investigation of buckling strength of longitudinally stiffened web of plate girders subjected to bending

Hee Soon Kim[1a], Yong Myung Park*[1], Byung Jun Kim[1b] and Kyungsik Kim[2c]

[1]*Department of Civil Engineering, Pusan National University, Busan 46241, Republic of Korea*
[2]*Department of Civil Engineering, Cheongju University, Cheongju 28503, Republic of Korea*

(Received December 15, 2017, Revised December 17, 2017, Accepted December 18, 2017)

Abstract. In this study, the bend-buckling strength of the web in longitudinally stiffened plate girder was numerically investigated. The buckling strength of the reinforced web was evaluated through an eigenvalue analysis of the hypothetical model, in which the top and bottom junctions of the web to the flanges were assumed as simple support conditions. Major parameters in the analysis include asymmetrical cross-sectional property, aspect ratio of the web, stiffener locations, and bending rigidity of the stiffeners. The numerical results showed that current AASHTO LRFD specifications (2014) provides the buckling strength from considerably safe side to slightly unsafe side depending on the location of the stiffeners. A modified equation for buckling coefficients was proposed to solve the shortcomings. The bending rigidity requirements of longitudinal stiffeners stipulated in AASHTO were also investigated. It is desirable to increase the rigidity of the stiffeners when the aspect ratio is less than 1.0.

Keywords: plate girder; longitudinal stiffener; in-plane bending; web bend-buckling strength; rigidity of stiffener

1. Introduction

In general, it is economical to make web as thin-walled as possible in the plate girder design because the section design of the girders is typically governed by bending moments rather than shear forces. However, the width-to-thickness ratio of the web must be properly controlled to prevent web bend-buckling, an elastic buckling of the web in compression due to in-plane bending, which can cause a considerable reduction of the bending resistance. To improve the strength of webs against bend-buckling, particularly if their slenderness ratios are very high, flat plate-shaped single-sided longitudinal stiffeners are commonly applied as shown in Fig. 1. Longitudinal stiffeners in a web can prevent the reduction of bending strength of the plate girders by controlling the lateral deflection of the web (Cooper 1967, Dubas 1948, Massonnet 1954, Rockey 1958, Rockey and Leggett 1962). Additionally, these stiffened web panel systems provide improved rotational restraint to the compression flanges and consequently resulting in increased bending strength (Ziemian 2010, Park *et al.* 2016). For the stiffened webs to be employed in plate girder bridges, a rational procedure for determining the buckling strength of the plate should be provided; the longitudinal stiffeners should have an appropriate rigidity to secure the estimated buckling strength of the considered plate girder.

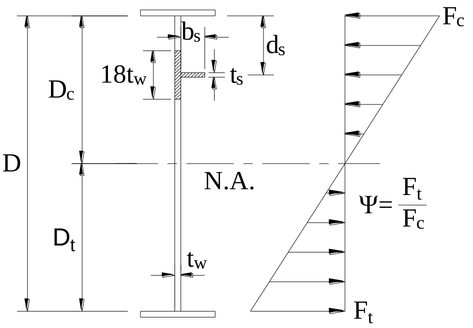

Fig. 1 Web with flat plate shaped single-sided longitudinal stiffener and effective T-section

Dubas (1948) suggested $0.2D$ (where D is the web depth) from the compression flange as the optimum location when a single longitudinal stiffener is provided in a symmetric girder, where the top and bottom junctions on the flanges were considered as simple support conditions. In this case, the buckling coefficient, k, of the web was obtained as 129.3 assuming that the bending stiffness is finite and the torsional rigidity is negligible for the longitudinal stiffeners. Meanwhile, Rockey and Leggett (1962) considered the top and bottom junctions of the web and the flange to be provided with clamped support condition. They suggested that the optimum location of a single longitudinal stiffener was $0.22D$ away from the compressive flange, and then the buckling coefficient increased to 161. Cooper (1967) performed a series of

*Corresponding author, Professor
E-mail: ympk@pusan.ac.kr
[a]Ph.D. Candidate
E-mail: kheesoon@hanmail.net
[b]Ph.D. Student
E-mail: bjun1300@pusan.ac.kr
[c]Associate Professor
E-mail: kkim@cju.ac.kr

ISSN: 1225-4568 (Print), 1598-6217 (Online)

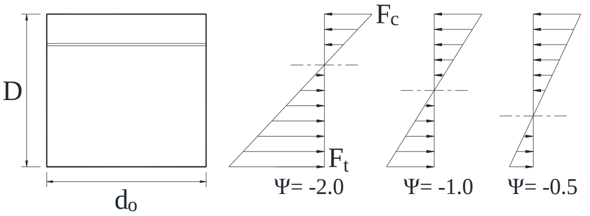

Fig. 2 Aspect ratio (d_o/D) and stress ratio (Ψ)

experiments for built-up beams with an yield strength of 230 MPa and the web slenderness ratios of up to 400-450. After completing the flexural strength tests, he concluded that the stresses at compression flanges could reach the yield strength under the condition that longitudinal stiffeners are provided with a certain level of required rigidity.

Thereafter, along with the development of computational analysis techniques, numerical studies on the ultimate buckling strength of longitudinally stiffened web systems were conducted by various researchers such as Azhari and Bradford (1993), Frank and Helwig (1995), Alinia and Moosavi (2008), Maiorana *et al*. (2011), Cho and Shin (2011), Shin *et al*. (2013), and Issa-EI-Khoury *et al*. (2014). Frank and Helwig proposed a refined expression for the optimum location of the stiffener, when simply supported web panels were assumed. Based on their study, they concluded that the optimum location of the single longitudinal stiffener could be expressed as $d_s/D_c = 0.4$, regardless of the asymmetry of the girder cross sections. The symbols d_s and D_c are the distance between the stiffener and the inner surface of the compression flange and the depth of web in compression in the elastic range, respectively, as shown in Fig. 1. Furthermore, the buckling coefficients of the stiffened webs were proposed separately for cases when $d_s/D_c \geq 0.4$ and when $d_s/D_c < 0.4$, which have been adopted by the current edition of AASHTO LRFD bridge design specifications (2014).

Longitudinal stiffeners act against compression force in combination with an adjacent strip of the web, resulting in an equivalent T-section shown in Fig. 1. Such a T-section is required to have sufficient rigidity to suppress the out-of-plane deformation of webs, i.e., to form the nodal line that is defined as a horizontal line of near zero lateral deflection in the web panel to resist bend-buckling (Bleich 1952, Timoshenko 1963). With regard to the rigidity of the longitudinal stiffener necessary to form nodal lines, Dubas (1948) and Massonett (1954) suggested guidelines in the range of web aspect ratio, α ($= d_o/D$ as shown in Fig. 2), $0.5 \leq \alpha \leq 1.5$ and $0.5 \leq \alpha \leq 1.6$, when a single longitudinal stiffener is located at $0.20D$.

Furthermore, prevention of lateral buckling of the equivalent T-section is also essential. Cooper (1967) derived the required radius of gyration of the T-section based on the strength equation for the lateral-torsional buckling, which was originally proposed by Basler and Thürlimann (1961). Cooper assumed in his work that the T-section is a simply supported column between the two adjacent locations where transverse stiffeners are present. The current version of AASHTO LRFD specifications has introduced the suggestions of Massonett (1954) and Cooper (1967) for the requirements of longitudinal stiffeners.

The main purpose of this study is to propose a modified equation for determining the buckling coefficients of web panels stiffened by a flat shaped single-sided longitudinal stiffener in symmetric and asymmetric cross section plate girders under in-plane bending. The web panel was assumed as an isolated stiffened plate system with simple support conditions that is the same schematics as AASHTO LRFD specifications. Comprehensive parametric eigenvalue analyses were conducted for a quantitative evaluation of the buckling coefficients. The major parameters in this study are stress ratio (the ratio of compressive stress to tensile stress), aspect ratio of the web, location, and rigidity of a single longitudinal stiffener. In addition, requirements for the rigidity of the longitudinal stiffeners to appropriately suppress the web bend-buckling in terms of the aspect ratios were analyzed. To this end, the required rigidity was investigated with the following aspects; achievement of the prescribed buckling strength of the web plate and prevention of lateral buckling of the equivalent T-section column.

2. Review of current design specifications

2.1 AASHTO LRFD specifications

In the AASHTO LRFD specifications (2014), the nominal bend-buckling resistance of a web (F_{crw}), which is based on the theoretical plate buckling resistance, is expressed as follows

$$F_{crw} = \frac{0.9kE}{(\frac{D}{t_w})^2} \quad (1)$$

where, *k* is the buckling coefficient, *E* is the elastic modulus of steel, and t_w is the thickness of the web, respectively. Based on Eq. (1), the Eq. (2) presents the limit of the slenderness ratio of stiffened webs at which F_{crw} reaches the yield strength of compression flange (F_{yc}). The stiffened webs, which satisfy this limit, are considered effective through the whole depth until the yield moment is reached, i.e., they are regarded to be non-compact webs (AASHTO 2014).

$$\frac{D}{t_w} \leq 0.95\sqrt{\frac{kE}{F_{yc}}} \quad (2)$$

The buckling coefficients of longitudinally stiffened webs in the AASHTO LRFD specifications were originated from Frank and Helwig (1995). They conducted a series of eigenvalue analyses using a simply supported web model with an aspect ratio of 1.0 (The model will be described in the section 3). The buckling coefficient equations were proposed through a curve fitting of their numerical results as follows

$$\frac{d_s}{D_c} \geq 0.4 \ : \ k = 5.17(\frac{D}{d_s})^2 \quad (3a)$$

$$\frac{d_s}{D_c} < 0.4 \; : \; k = 11.64\left(\frac{D}{D_c - d_s}\right)^2 \tag{3b}$$

AASHTO LRFD stipulates the dimension and rigidity of the longitudinal stiffeners as follows. The specifications limit the width-to-thickness ratio, as shown in Eq. (4), to prevent the local buckling of the longitudinal stiffener.

$$b_s \leq 0.48 t_s \sqrt{\frac{E}{F_{ys}}} \tag{4}$$

where, b_s is the width of the longitudinal stiffener, t_s is the thickness of the longitudinal stiffener, and F_{ys} is the yield strength of the longitudinal stiffener. As a rigidity requirement for the longitudinal stiffener against the out-of-plane deformation of the web, i.e., to form the nodal line in the web plate, the required moment of inertia for the T-section should satisfy Eq. (5). As shown in Fig. 1, the T-section consists of the effective width $18t_w$ in the web portion and the cross-sectional area of the longitudinal stiffener.

$$I_l \geq D t_w^3 \left[2.4\left(\frac{d_o}{D}\right)^2 - 0.13\right]\beta \tag{5}$$

where, I_l is the moment of inertia of the T-section with respect to its neutral axis, d_o is the spacing of transverse stiffeners, and β is the curvature correction factor for curved girders that is 1.0 for straight girders.

Furthermore, based on the suggestions by Cooper (1967), a limit for the radius of gyration of the T-section is set, as presented in Eq. (6), to withstand axial compressive stress without lateral buckling.

$$r_s \geq \frac{0.16 d_o \sqrt{\frac{F_{ys}}{E}}}{\sqrt{1 - 0.6\frac{\mathrm{F_{yc}}}{\mathrm{R_h} F_{ys}}}} \tag{6}$$

where, r_s is the radius of gyration of the T-section with respect to its neutral axis and R_h is the hybrid factor applied to hybrid cross sections (AASHTO 2014).

2.2 Eurocode 3

EN 1993-1-5 of Eurocode 3 (CEN 2006) specifies that the flexural strength of the girder sections can be determined by considering the effective widths of the compressive flange and the reinforced web, which are dependent on the buckling strengths of the plate elements. For a stiffened web, the buckling strengths and the corresponding effective widths of the web are calculated by considering the individual sub-panels divided by a longitudinal stiffener, i.e., the upper and the lower panels, which are assumed as simple supports at the locations of the flanges and the longitudinal stiffener. The design philosophy for buckling strengths specified in Eurocode 3 is intrinsically different from that defined in the AASHTO LRFD specifications. This study is focused on the review of AASHTO stipulations.

Table 1 Parameters considered in this study

Parameter	Range
$\Psi(= F_t/F_c)$	-2.0, -1.5. -1.0(symmetric), -0.75, -0.5, -0.33
$\alpha(= d_o/D)$	0.33 - 2.5
d_s/D_c	0.25, 0.3, 0.35, 0.4, 0.45, 0.5, 0.55
γ	Min. 5(α = 0.33), Max. 250(α = 2.5)

3. Numerical analysis

3.1 Parameters

Major parameters and their corresponding ranges considered in this study are summarized in Table 1. First, the asymmetry of the hypothetical girder sections was considered with the stress ratio $\Psi\ (= F_t/F_c)$, as shown in Fig. 2, where F_c is the compressive stress (positive value) on the top of the web and F_t is the tensile stress (negative value) on the bottom of the web. The cross-sectional area of the compressive flange (A_{fc}) is smaller than that of the tension flange (A_{ft}) in the positive moment zones while A_{fc} is proportioned similar or a little greater than A_{ft} in the negative moment zones in most practical plate girder bridges with a concrete deck. The stress ratios were chosen in the range of -2.0 to -0.33 to take into account a certain degree of asymmetry.

If the aspect ratio(α) becomes larger, i.e., if the spacing of transverse stiffeners(d_o) increases, the dimensions of the longitudinal stiffener will be larger, which will be less economical with respect to the weight of the used material. In addition, the aspect ratios in practical designs hardly exceeds 2.0 since shear force and bending moment are acting simultaneously in most sections of the bridges. The aspect ratios considered in this study were in the range of 0.33 to 2.5.

The stiffener locations are presented by the ratio of d_s/D_c. In the case where a single longitudinal stiffener is installed, the optimum stiffener location in the simply supported web model was found as $d_s/D_c = 0.4$ regardless of the asymmetry of the girder sections as stated earlier. In many practical designs, the stiffeners are installed at the $0.2D$ location as a rule of thumb even in the asymmetric sections. In the asymmetric sections, the location ratio, d_s/D_c, will be greater than 0.4 if $A_{fc} > A_{ft}$ and smaller than 0.4 if $A_{fc} < A_{ft}$ when the stiffeners are uniformly installed at $0.2D$. Therefore, the ratio d_s/D_c was varied from 0.25 to 0.55 for the hypothetical models.

The rigidity of stiffener was considered in the form of a rigidity ratio (γ), which is defined as the ratio of the bending rigidity of the stiffener to that of the web as expressed in Eq. (7).

$$\gamma = \frac{E I_l}{D D_{plate}} \tag{7}$$

where, $D_{plate} = E t_w^3 / 12(1 - \nu^2)$ is the bending rigidity of web and ν is the Poisson's ratio of steel (=0.3). The

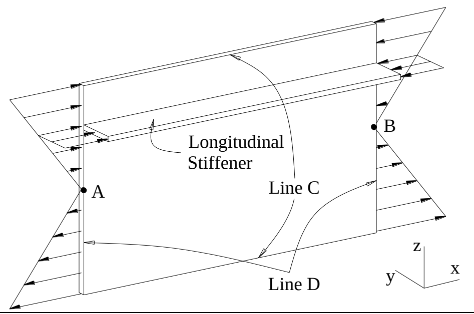

Location	Dx	Dy	Dz	Rx
Point A	Fix	-	Fix	-
Point B	-	-	Fix	-
Line C	-	Fix	-	Fix*
Line D	-	Fix	-	-

* only for clamped web model

(a) Model without flange

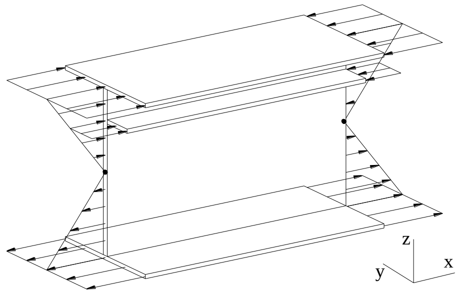

(b) Model with flanges

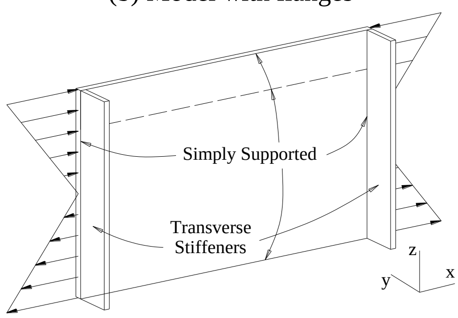

(c) Frank and Helwig’s model

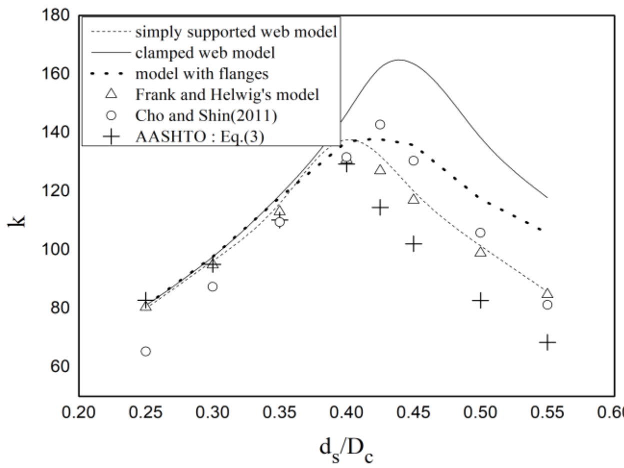

(d) Variations of buckling coefficients with d_s/D_c depending on numerical models ($\Psi = -1$, $\alpha = 1.0$, and $\gamma = 30$: $b_s \times t_s = 120 \times 13.3$ mm)

Fig. 3 Numerical models and results of buckling coefficients

rigidity ratio was varied from 5 up to 250 depending on the aspect ratios in this study.

When the cross-sectional area of the stiffener is kept constant, the buckling strength of the stiffened web slightly increases as the width-to-thickness ratio of the longitudinal stiffener(b_s/t_s) increases up to the limit of the slenderness ratio, given in Eq. (4) (Kim 2013). However, the degree of increase is minor, so the ratio b_s/t_s was not included in the parametric analyses and assumed to be between 9.0 and 10.0 in the following analyses.

3.2 Numerical model

The buckling strengths of the stiffened web panels subjected to the in-plane bending action were evaluated through eigenvalue analyses. Prior to the numerical analyses on the major parameters, a preliminary analysis was conducted to investigate the effect of constraining the web rotation by the flanges. A symmetric cross section model ($\Psi = -1.0$) was considered for three types of support conditions; a simple support, a clamped support, and an elastic support by flanges. The depth and the thickness of the hypothetical webs were assumed as 2,000 mm and 10 mm, respectively. Fig. 3(a) shows the web model without flanges and the support conditions. The simply supported model was considered to have simple supports at the upper and lower flange locations (Line C in Fig. 3(a)), which neglect the constraining effect by the flanges. The clamped model was considered by additionally restraining the rotations along the Line C, which might correspond to the cases when the flanges are very thick. Fig. 3(b) shows the model with flanges, and the width and the thickness of the flanges were assumed to be 500 mm and 20 mm, respectively.

The transverse stiffeners were not included in the model and both vertical edges of the web were assumed to be simply supported (Line D in Fig. 3(a)) for all the models. These conditions may lead subsequent buckling strengths to the conservative side. The in-plane bending action of the web plate was simulated with compressive and tensile stress gradients on both ends of the web as shown in Fig. 3(a) and (b). It should be noted that corresponding compressive stresses at the stiffener location were also applied to the entire cross section of the longitudinal stiffener. For the model with flanges, compressive and tensile stresses were applied to the flanges as shown in Fig. 3(b).

In addition, the numerical model by Frank and Helwig (1995) was analyzed for comparison purpose. The scheme of their model is shown in Fig. 3(c). The four edges of the web were assumed as simple support conditions and the transverse stiffeners were also included in the model. The longitudinal stiffener was represented by fixing the nodes of the web against the out-of-plane deformation at the stiffener locations, instead of explicitly modeling them with plate elements. This implies that the longitudinal stiffeners are assumed to have sufficient flexural rigidity.

3.3 Validation of numerical model

The eigenvalue analyses were performed using the ABAQUS software package (2014). The S4R 4-node shell

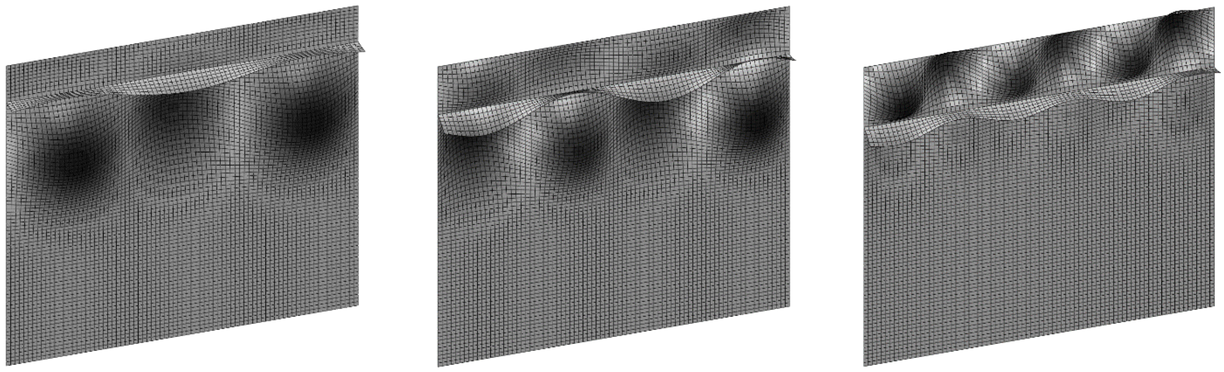

$d_s/D_c = 0.3(k = 148.1)$ $d_s/D_c = 0.4(k = 214.1)$ $d_s/D_c = 0.5(k = 158.2)$

(a) $\Psi = -1.5$

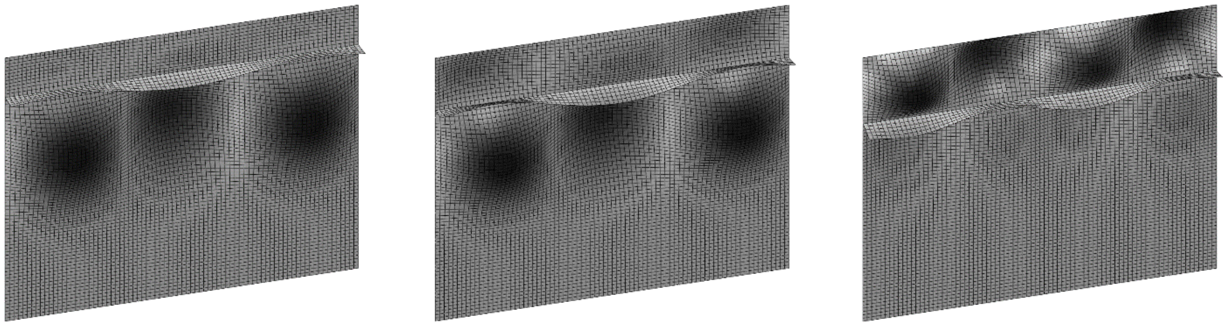

$d_s/D_c = 0.3(k = 96.2)$ $d_s/D_c = 0.4(k = 137.6)$ $d_s/D_c = 0.5(k = 101.4)$

(b) $\Psi = -1.0$

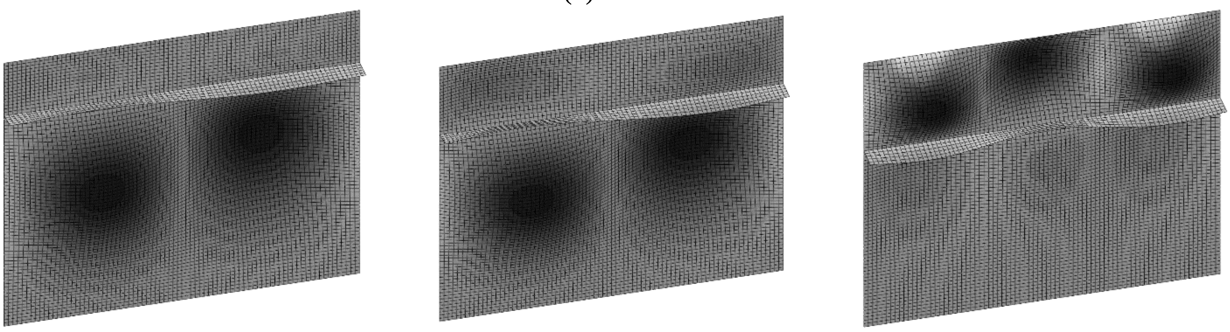

$d_s/D_c = 0.3(k = 52.9)$ $d_s/D_c = 0.4(k = 78.2)$ $d_s/D_c = 0.5(k = 56.9)$

(c) $\Psi = -0.5$

Fig. 4 Buckling mode shapes vs. d_s/D_c and Ψ ($\alpha = 1.0,\ \gamma = 30$: $b_s \times t_s = 120 \times 13.3$ mm)

Table 2 Values of buckling coefficients ($\boldsymbol{k}$) obtained from various numerical models ($\boldsymbol{\Psi = -1.0, \alpha = 1.0}$)

d_s/D_c		0.25	0.3	0.35	0.4	0.425	0.45	0.5	0.55
This study ($\gamma = 30$: $b_s \times t_s = 120 \times 13.3$ mm)	Simply Supported web model	80.0	96.2	115.8	137.6 (129.3)	132.1	120.1	101.4 (101.0)	85.7
	Clamped web model	81.0	97.7	118.7	146.5 (142.6)	162.1	163.5 (161.0*)	138.3	117.8
	Model with flange	80.9	97.6	117.8	137.0	137.7	135.7	117.4	105.7
Frank and Helwig's model		80.4	94.9	113.0	130.7	127.0	117.0	98.9	84.7
AASHTO LRFD: Eq. (3)		82.8	95.0	110.2	129.3	114.5	102.1	82.7	68.4
Cho and Shin (2011)		65.3	87.4	109.5	131.6	142.7	130.4	105.8	81.2

Note: The values in the parenthesis are theoretical buckling coefficients and $k = 161.0^*$ is for $d_s/D_c = 0.44$

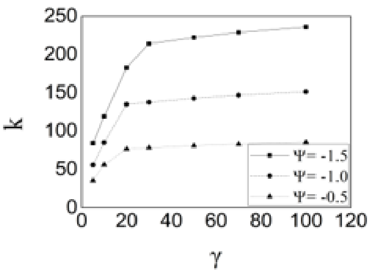

Dim. of stiffeners

γ	$b_s \times t_s$
5	70×7.8
10	86×9.6
20	106×11.8
30	120×13.3
50	140×15.6
70	156×17.2
100	174×19.2

Fig. 5 Example of convergence curves according to γ ($\alpha = 1.0,\ d_s/D_c = 0.4$)

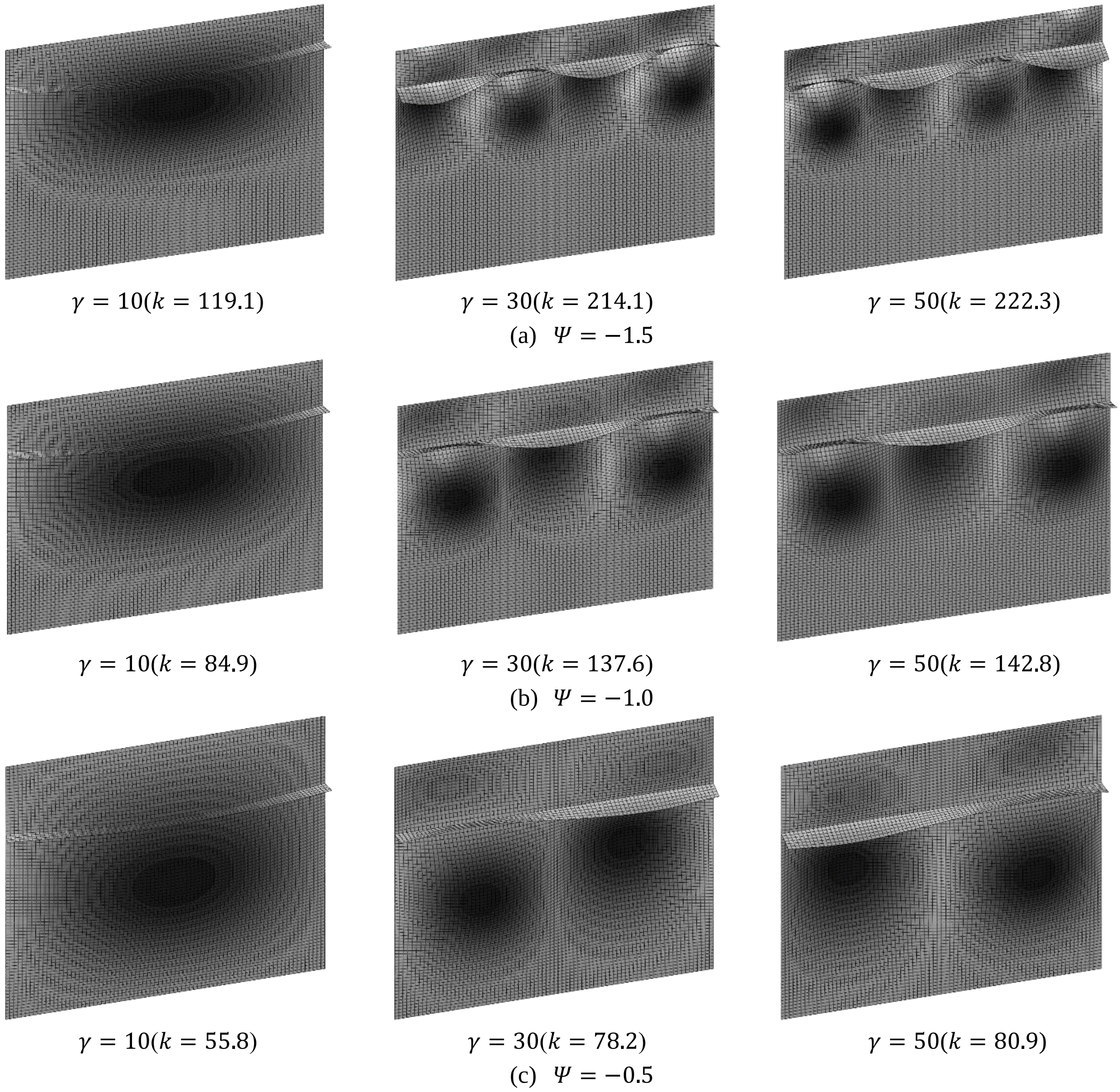

Fig. 6 Buckling mode shapes vs. γ ($\alpha = 1.0,\ d_s/D_c = 0.4,\ \gamma = 10 : b_s \times t_s = 86 \times 9.6\ mm,\ \gamma = 30 : 120 \times 13.3\ mm,\ \gamma = 50 : 140 \times 15.6\ mm$)

elements were employed for the modelling of the plates.

The web plate was divided into 80 elements in depth, and the aspect ratio of each element was set as close to 1.0 as possible. The stiffeners were also divided so that their mesh dimensions might be similar to those of the web plate. In the model with flanges, the flanges were divided into 20 elements in width to maintain the size of each element similar to that of the web plate.

The resultant buckling coefficients for three support conditions, when $\alpha = 1.0$ and $\gamma = 30(b_s \times t_s = 120 \times 13.3\ \text{mm})$, are presented depending on the stiffener locations (d_s/D_c) in Table 2 and Fig. 3(d). The theoretical values of buckling coefficients obtained from the previous studies (Dubas 1948, Rockey and Leggett 1962, Bleich 1952), those obtained from Frank and Helwig's model, those calculated by using Eq. (3) under AASHTO LRFD specifications, and those calculated from the design equation by Cho and Shin (2011) shown in Eq. (8) are presented together.

$$\frac{d_s}{D_c} \geq 0.425\ :\ k = (88 - 123.1\frac{d_s}{D_c})(\frac{D}{D_c})^2 \tag{8a}$$

$$\frac{d_s}{D_c} < 0.425\ :\ k = (110.6\frac{d_s}{D_c} - 11.33)(\frac{D}{D_c})^2 \tag{8b}$$

The simply supported web model and the clamped web model considered in the present study reasonably well estimate the buckling coefficients compared with the theoretical values. Furthermore, the simply supported model provided very similar buckling coefficients to those from Frank and Helwig's model. However, Eq. (3) provided considerably lower values of buckling coefficients when $d_s/D_c > 0.4$ and critical values as d_s/D_c becomes smaller than 0.4. Meanwhile, Eq. (8) which was derived

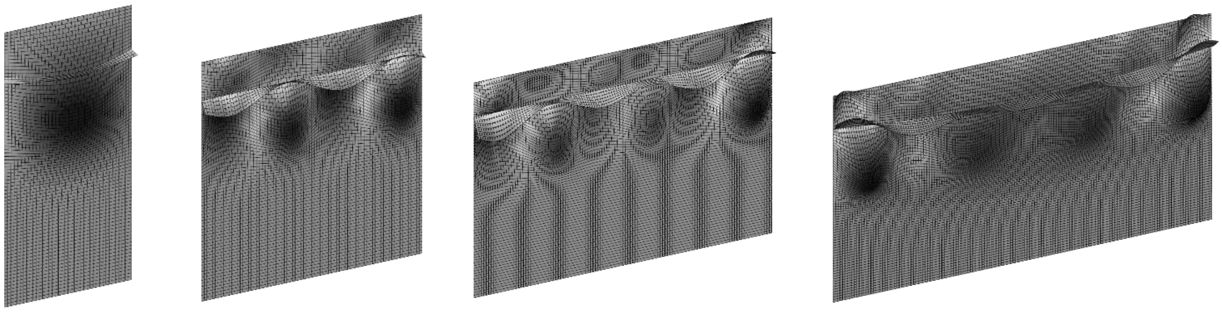

($k = 153.7$) ($k = 211.7$) ($k = 226.7$) ($k = 236.2$)

(a) $\Psi = -1.5$: $\alpha = 0.5, 1.0, 1.5, 2.0$

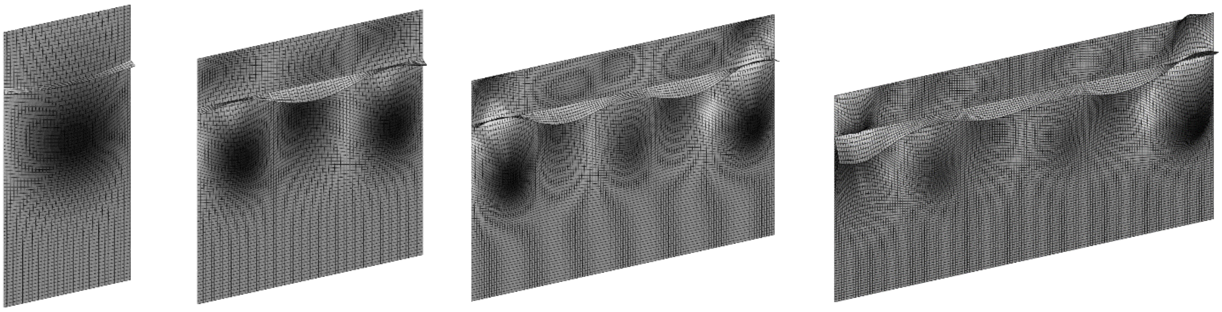

($k = 110.6$) ($k = 136.0$) ($k = 146.6$) ($k = 152.5$)

(b) $\Psi = -1.0$: $\alpha = 0.5, 1.0, 1.5, 2.0$

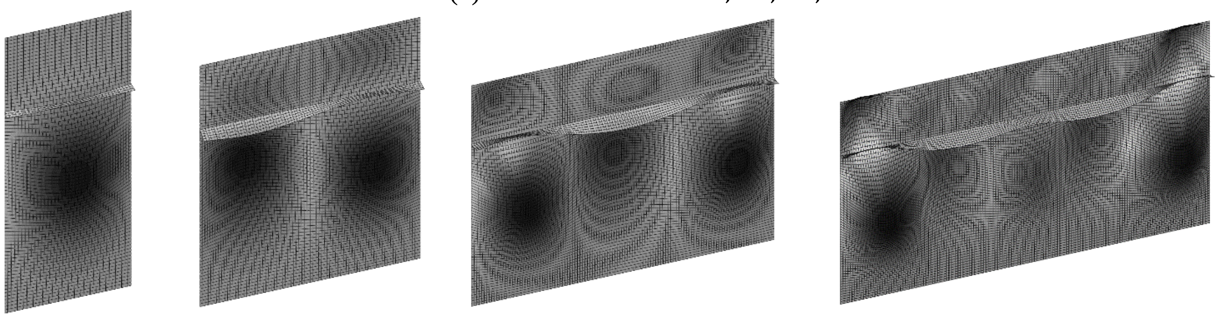

($k = 68.2$) ($k = 77.4$) ($k = 82.6$) ($k = 87.4$)

(c) $\Psi = -0.5$: $\alpha = 0.5, 1.0, 1.5, 2.0$

α	0.5	1.0	1.5	2.0
γ_{AASHTO} : Eq. (5)	5.1	24.8	57.5	103.4
$b_s \times t_s$	71×7.8	113×12.6	146×16.3	176×19.4

Fig. 7 Buckling mode shapes vs. α ($d_s/D_c = 0.4$)

based on the girder models with flanges provides the buckling coefficients between simply supported and clamped web model when $d_s/D_c > 0.4$.

Fig. 3(d) illustrates that the optimum location of the stiffener moves from $0.4D_c$ to $0.45D_c$ as the flange became thicker. Therefore, the optimum location of the longitudinal stiffener in actual girders is expected to exist between $0.4D_c$ and $0.45D_c$. The simply supported web model was employed for the following numerical analyses since it yielded the smallest buckling coefficient.

4. Numerical results of buckling analysis

4.1 Buckling modes

4.1.1 Buckling modes versus stiffener locations and stress ratios

Fig. 4 shows the buckling mode shapes and the corresponding buckling coefficients for typical cases. A total of nine mode shapes in Fig. 4 represent combinations of three different stress ratios ($\Psi = -1.5$, -1.0, and -0.5) and three different stiffener locations ($d_s/D_c = 0.3, 0.4,$ and 0.5). It is noted that α and γ were set as 1.0 and 30, respectively. It can be confirmed that the plate buckling occurs in the lower panel when $d_s/D_c < 0.4$ and in the upper panel when $d_s/D_c > 0.4$ regardless of the stress ratio. When $d_s/D_c = 0.4$, anti-symmetric mode shape with respect to the stiffener location, i.e., simultaneous buckling is detected in the upper and lower panels, which results in the highest buckling strength. Also, the number of half-waves and the buckling coefficient increase as the stress ratio attains a smaller value under the same stiffener location.

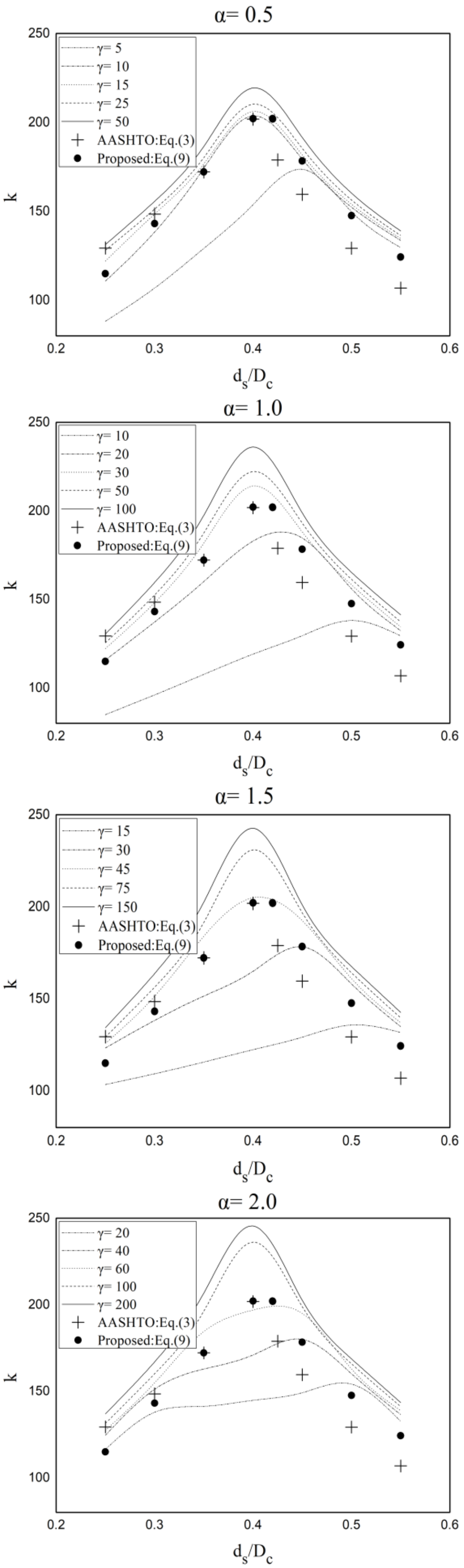

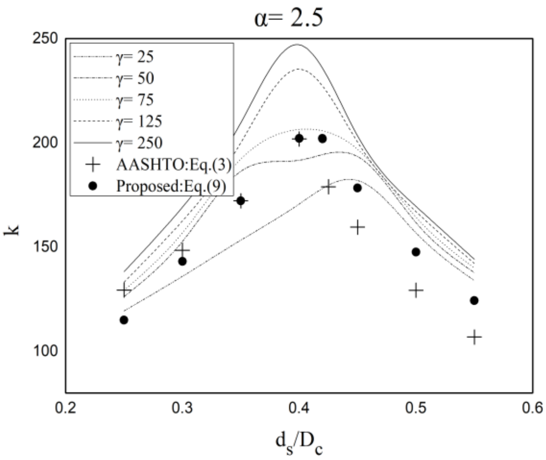

(a) $\Psi = -1.5$

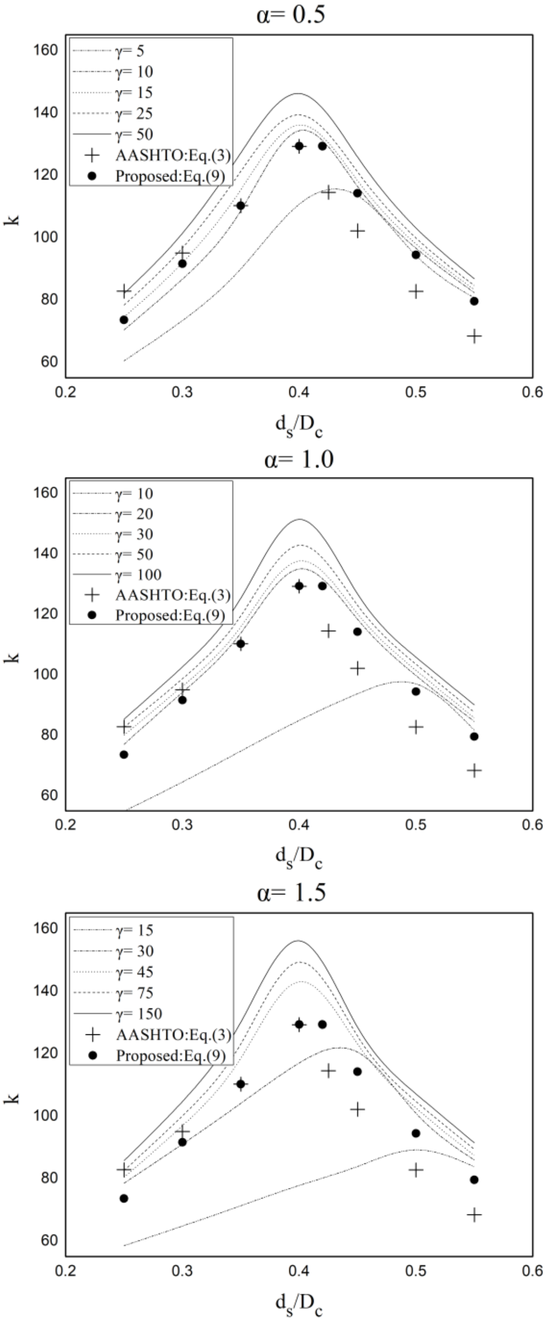

Fig. 8 Buckling coefficients vs. $\alpha, d_s/D_c, \Psi$ and γ

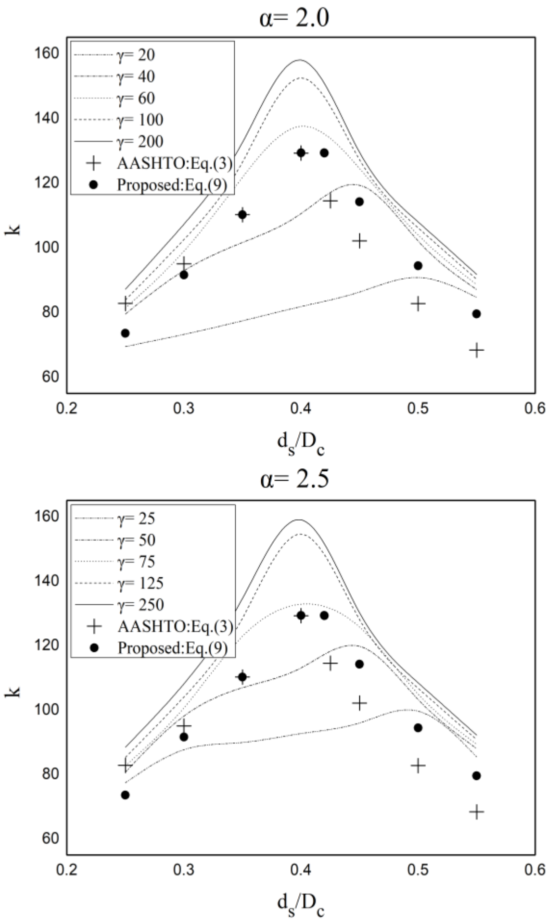

(b) $\Psi = -1.0$

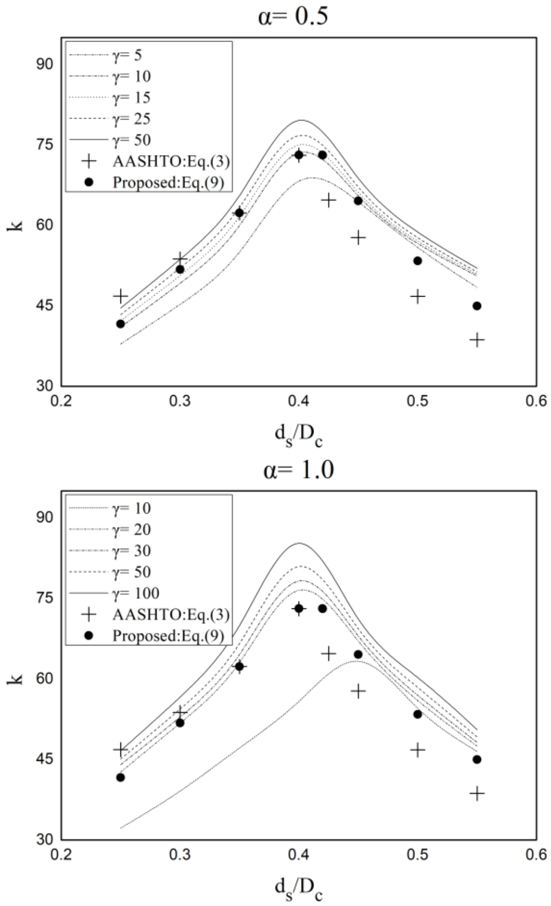

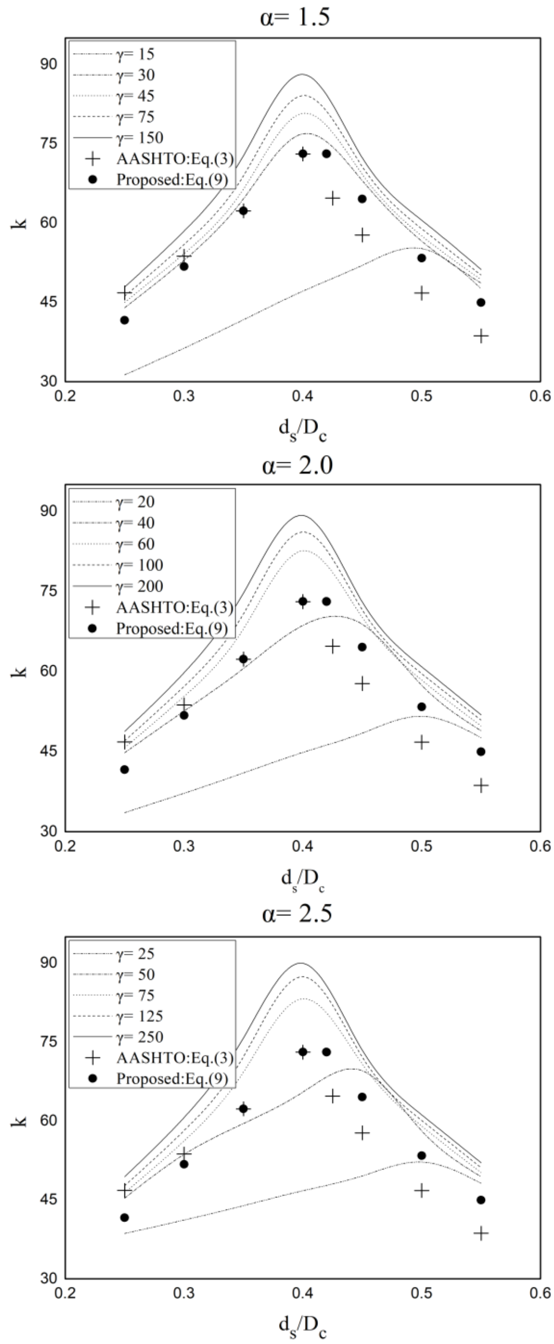

(c) $\Psi = -0.5$

Fig. 8 Continued

4.1.2 Buckling modes versus rigidity ratios

Fig. 5 presents the variations of k with increase in γ, under $\alpha = 1.0$ and $d_s/D_c = 0.4$ for three different stress ratios ($\Psi = -1.5,\ -1.0,$ and -0.5). It is confirmed that k rapidly increases as the γ increases up to a certain value and then shows a very low or near-zero increment. This curve pattern, as stated in previous works (Maiorana *et al*. 2011, Issa-El-Khoury *et al*. 2014, Choi *et al*. 2009), represents a characteristic relationship between the buckling strength of the stiffened web and the rigidity of the installed stiffener.

Fig. 6 presents the buckling mode shapes and the corresponding buckling coefficients for the three different

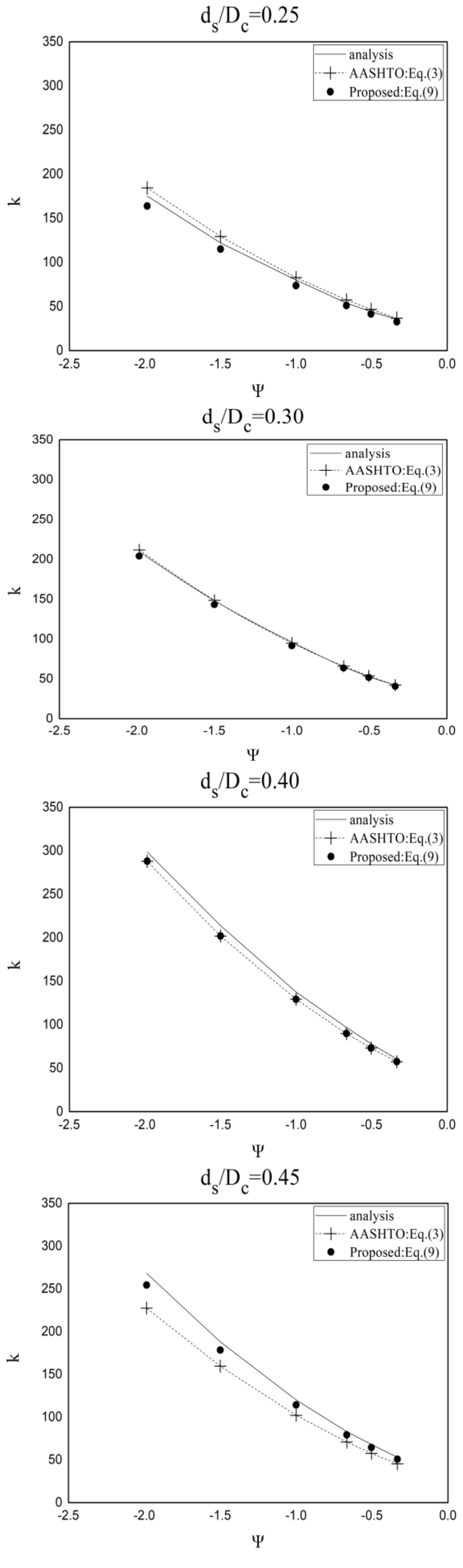

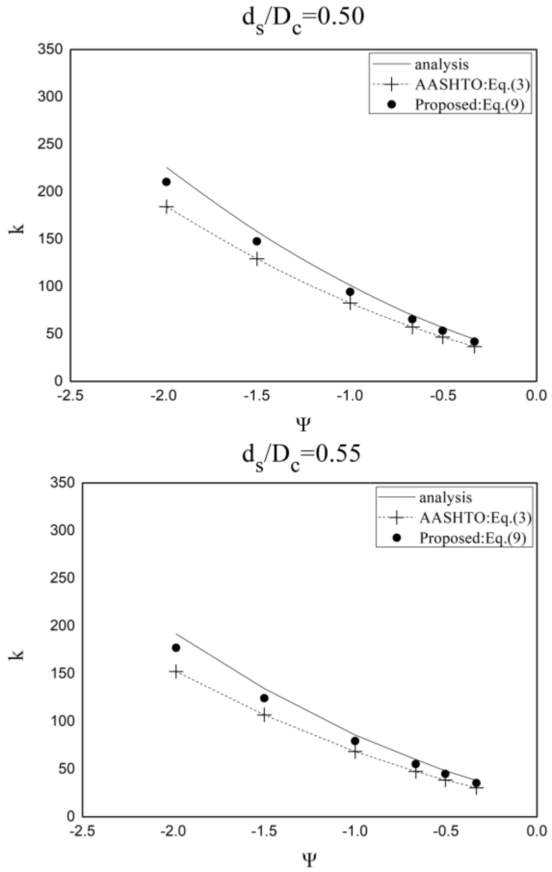

Fig. 9 Buckling coefficients vs. d_s/D_c and Ψ ($\alpha = 1.0$, $\gamma = 30$: $b_s \times t_s$=120×13.3 mm)

stress ratios ($\Psi = -1.5$, -1.0, and -0.5) and three different rigidity ratios ($\gamma = 10, 30, \text{and } 50$). Furthermore, α and the stiffener location, d_s/D_c, were set to 1.0 and 0.4, respectively. It can be observed that the stiffened web panels are subjected to the global plate buckling mode showing a single waveform when the rigidity ratio is 10, which is attributable to the insufficient rigidity of the stiffener. Mode shapes become more localized, retaining the straight nodal lines when the rigidity ratio is greater than the critical value. The number of half-waves is the same at $\gamma = 30$ and 50, implying that the buckling strength does not increase significantly even though the rigidity ratio is greater than the critical value. Therefore, it can be confirmed that the longitudinal stiffeners should have a certain degree of rigidity to suppress the global buckling mode and to result in a localized buckling mode ensuring the prescribed buckling strength (Choi *et al*. 2009).

4.1.3 Buckling modes versus aspect ratios

Fig. 7 shows the buckling modes and buckling coefficients according to aspect ratios (α). Similar to the previous condition, three different stress ratios ($\Psi = -1.5$, -1.0, and -0.5) were considered, while the stiffener location parameter (d_s/D_c) was set to be 0.4. The minimum I_l for a given α under AASHTO LRFD specifications (i.e., Eq. (5)) was applied; the rigidity ratio(γ) corresponding to the applied I_l is given in Fig. 7. It is observed that the number of half-waves in the buckling mode increases as the aspect ratio increases. The length of half-waves is about $0.33D$ when $\Psi = -1.0$ and $\alpha \geq 1.0$, which is a half of $0.66D$ developed in unstiffened webs (Rockey and Leggett 1962). It is further notable that the longitudinal stiffener cannot contribute to the formation of nodal lines owing to insufficient rigidity when $\alpha = 0.5$. The rigidity requirement for the longitudinal stiffener will be discussed in the section 6.

4.2 Resultant buckling strength

Fig. 8 shows the comprehensive results of the buckling coefficients according to the variation of four major parameters: Ψ, α, γ, and d_s/D_c. Although the buckling coefficients were not proposed yet in this study, Fig. 8 exhibits the plots in advance from the proposed equation shown in Eq. (9) that will be developed and presented later in section 5. The buckling coefficients derived from the AASHTO LRFD specifications, which are given in Eq. (3), are also shown together for comparison purpose. It is confirmed that the maximum buckling coefficient is obtained when d_s/D_c is equal to 0.4 regardless of stress ratios (Ψ). Furthermore, if the stiffeners possess a certain degree of rigidity, the buckling coefficients from the AASHTO LRFD specifications are generally in good agreement when $d_s/D_c = 0.4$ and on the considerably conservative side when $d_s/D_c > 0.4$ compared with those of this study. In the cases when $d_s/D_c < 0.4$, however, the specifications have a tendency to overestimate the buckling coefficients slightly as d_s/D_c becomes smaller, considering stiffener rigidity is not always guaranteed to be able to achieve the corresponding maximum value.

Furthermore, when $d_s/D_c < 0.4$, buckling occurs in the lower panel and the corresponding buckling strengths hardly increase even if the flange effect is taken into account as shown in Fig. 3(d). Therefore, the current AASHTO standards may lead to a critical or a slightly unsafe web thicknesses if applied to cases where the longitudinal stiffener is installed at $0.2D$ in the asymmetric sections with $A_{ft} > A_{fc}$.

It is generally accepted that a closed-section stiffener has a better performance than an open-sectioned one (Maiorana *et al.* 2011). It is noted that the flat plate longitudinal stiffener on single-side of web as shown in Fig. 1 was considered in this study and the results should be limited to the cases using the flat plate-shaped stiffeners.

5. Bend-buckling coefficients of longitudinally stiffened webs

5.1 Proposal of buckling coefficient formula

Fig. 8 demonstrates that the buckling coefficient mainly depends on the stiffener location (d_s/D_c) and the stress ratio (Ψ). By incorporating the two variables, the modified equations for buckling coefficient were derived in the form of $k = 10^{m_1}(d_s/D_c)^{m_2}(1-\Psi)^{m_3}$. The coefficients m_1, m_2 and m_3 were determined using a basic spread sheet program based on multi-variable regression analyses (Allison 1999) and new equations are proposed as follows

Table 3 Minimum web thickness required to prevent elastic buckling ($\boldsymbol{D = 2,000\ mm}$, $\boldsymbol{F_{yc} = 315\ MPa}$)

Ψ	D_c (mm)	d_s (mm)	$\frac{d_s}{D_c}$	AASHTO LRFD		This study	
				k	t_{min} (mm)	k	t_{min} (mm)
-1.5	800	400	0.5	129.3	7.3	147.6	6.8
-1.0	1000	400	0.4	129.3	7.3	129.3	7.3
-0.5	1330	400	0.3	53.8	11.3	51.7	11.5

$$d_s/D_c \geq 0.42 \ : \ k = 6.78\left(\frac{D_c}{d_s}\right)^{1.8}(1-\Psi)^2 \tag{9a}$$

$$d_s/D_c < 0.42 \ : \ k = 97.1\left(\frac{d_s}{D_c}\right)^{1.2}(1-\Psi)^2 \leq 32.33(1-\Psi)^2 \tag{9b}$$

Eqs. (9a) and (9b) reflected the result that the maximum buckling coefficients for the model with flanges are obtained when d_s/D_c is some around 0.42 as shown in Fig. 3(d). In addition, Eqs. (9a) and (9b) also consider the theoretical value of k as 129.3 in the symmetric section when $d_s/D_c = 0.4$ in the simply supported model. The buckling coefficients estimated from the proposed equations given in Eqs. (9a) and (9b) are also plotted as solid dots in Fig. 8. It is evident that the proposed formulae for k provide a reasonable evaluation of buckling strengths of longitudinally stiffened webs, reflecting the analyses results. As the rigidity of the stiffener (γ) was not included as a variable during the derivation of Eq. (9), these equations provide a lower bound of buckling coefficient.

The proposed buckling coefficients for the cases of $\alpha = 1.0$ and $\gamma = 30$ according to variation of d_s/D_c and Ψ are comparatively presented in Fig. 9. It is confirmed that the AASHTO LRFD specifications expect the buckling strengths to be generally on the conservative side in most cases. However, the buckling strengths are slightly overestimated by the specifications as d_s/D_c becomes smaller.

5.2 Sample comparison of minimum web thicknesses

Table 3 summarizes the minimum thicknesses of the web necessary to prevent elastic bend-buckling along with corresponding k calculated using the AASHTO LRFD specifications and the present study. For the comparison, three different stress ratios were considered while the location of the longitudinal stiffener was equally set at $0.2D$. The web depth is 2,000 mm, and the yield strength and elastic modulus are 315 MPa and 205 GPa, respectively.

It is noted that these two proposals expect the same values for k and the minimum thickness when $d_s/D_c = 0.4$. The AASHTO LRFD specifications provide the minimum thickness on more safe-side than the present study when $d_s/D_c > 0.4$. However, when $d_s/D_c < 0.4$,

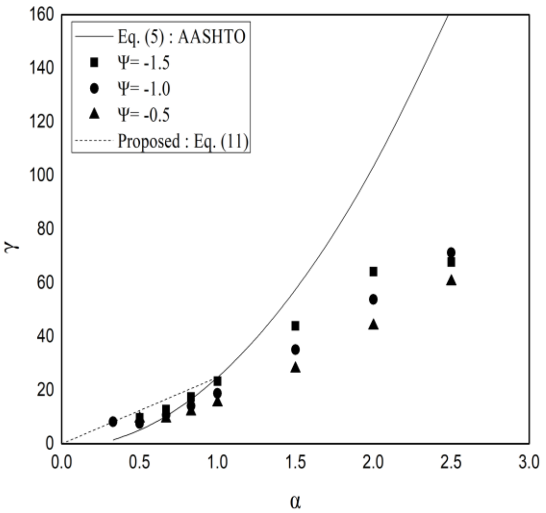

Fig. 10 Required γ to obtain prescribed k

the web thickness expected from the AASHTO LRFD specifications may be critical or slightly unsafe.

6. Required rigidity of longitudinal stiffeners

6.1 Rigidity to obtain prescribed buckling strength

Figs. 5 and 6 illustrated that a nodal line is formed and the buckling strength becomes close to the maximum value when the rigidity of longitudinal stiffeners is greater than a critical value. As stated before, Eq. (5) was adopted as a regulation for the moment of inertia of the equivalent T-section so that the longitudinal stiffener can form nodal lines against web bend-buckling. This is based on Eq. (10) proposed by Massonett (1954) for aspect ratios in the range of $0.5 \leq \alpha \leq 1.6$, derived based on the simply supported web model.

$$\gamma = 3.87 + 5.1\alpha + (8.82 + 77.6\delta)\alpha^2 \quad \text{for } 0.5 \leq \alpha \leq 1.6 \tag{10}$$

where, $\delta = A_s / D t_w$ and A_s is the cross-sectional area of longitudinal stiffener.

Fig. 10 shows the minimum γ values required to obtain the proposed buckling coefficients given in Eq. (9) as α varies. It is indicated that a higher γ is required as Ψ becomes smaller. When Ψ is less than -1.0, i.e., $D_c < D_t$, the required γ may be reduced because tension flanges will be subjected to yielding prior to the failure of compression flanges. However, such an assumption was not considered in Fig. 10. The solid line, denoted as AASHTO in the legend of Fig. 10, represents the rigidity ratios calculated from the minimum moment of inertia of the T-section, I_l, given by Eq. (5). It can be found that the moment of inertia in Eq. (5) under the AASHTO LRFD specifications is insufficient to ensure the required web buckling strength when $\alpha < 1.0$. This explains why global plate buckling modes were exhibited without the formation of nodal lines when $\alpha = 0.5$ as shown in Fig. 7. It is noted that the minimum I_l, which is given by Eq. (5) under AASHTO specification, was applied to all models in Fig. 7.

Table 4 Required rigidity ratio of longitudinal stiffener $(\boldsymbol{D = 2,000\ mm,\ t_w = 12\ mm})$

		α	0.33	0.50	0.67	0.83	1.0	1.5	2.0	2.5
γ_{req} from Eq. (5)			1.4	5.1	10.3	16.6	24.8	57.5	103.4	162.4
γ_{req} from Eq. (6)	$F_{yc} = 315MPa$	$F_{ys} = 210MPa$	1.1	2.6	5.0	8.1	12.7	37.0	87.5	184.6
		$F_{ys} = 315MPa$	0.4	0.9	1.7	2.7	4.0	10.4	21.4	39.5
	$F_{yc} = 690MPa$	$F_{ys} = 450MPa$	3.0	7.8	16.0	27.8	46.9	172.3	501.1	1,217.0
		$F_{ys} = 690MPa$	0.9	2.1	3.9	6.4	10.0	27.8	63.9	130.8

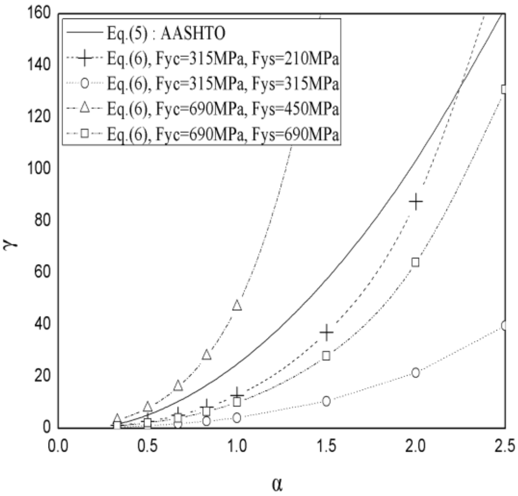

Fig. 11 Required γ to prevent buckling of T-section

Meanwhile, it is observed from Fig. 10 that the required γ values under AASHTO are greater than those for ensuring the prescribed buckling strength as α becomes larger than 1.0. Rockey and Leggett (1962) reported that the required rigidity of the stiffener in the clamped web model decreases greatly as compared to the simply supported condition when α becomes larger than 1.0. Since the post-buckling strength will increase as the rigidity of the longitudinal stiffener increases (Rockey 1958), the rigidity requirement in the current AASHTO LRFD specifications is considered to be applicable as the safe side in cases where $\alpha > 1.0$. However, in cases where $\alpha < 1.0$, the lower bound needs to be re-established. The authors assumed that the required $\gamma = 24.8$ at $\alpha = 1.0$; corresponding to the minimum requirement of current AASHTO LRFD specifications, and $\gamma = 0$ at $\alpha = 0$, as presented with a dotted line in Fig. 10. Then, the required γ is represented as a linear function, and a simple conversion for the required moment of inertia for the T-section yields

$$I_{l,\min} \geq D t_w^3 \left[2.27 \left(\frac{d_0}{D} \right) \right] \quad \text{for } \alpha < 1.0 \tag{11}$$

6.2 Rigidity to prevent buckling of T-section

Eq. (6) was proposed as a regulation to prevent the lateral buckling of the equivalent T-section (Cooper 1967). In this methodology, the required radius of gyration of the

T-section, r_s, depends on the spacing of transverse stiffener (d_o), the yield strength of compression flange (F_{yc}) and longitudinal stiffener (F_{ys}). For a specified d_o, the required r_s increases as F_{yc} increases and F_{ys} decreases. To investigate the required r_s, two types of F_{yc}, 315 MPa and 690 MPa, are considered for the compression flanges. A lower yield strength steel is often used for the longitudinal stiffeners in practices because the maximum compressive stress at the stiffener location is around 60% of the compression flange. Therefore, two types of F_{ys}, 210 MPa and 315 MPa for the case of F_{yc} =315 MPa, and 450 MPa and 690 MPa for the case of $F_{yc} = 690$ MPa, respectively, are considered for the longitudinal stiffeners. A web of $D = 2{,}000$ mm, $t_w = 12$ mm, and homogeneous girder section ($R_h = 1.0$) is assumed.

Table 4 and Fig. 11 present the required rigidity ratios which are recalculated from Eq. (6) for $0.33 \leq \alpha \leq 2.5$, in which the rigidity ratios based on Eq. (5) are also shown. Table 4 and Fig. 11 show that Eq. (5) governs the required rigidity when the yield strength of the stiffener is equal to that of the compression flange for the considered range of α and yield strength of steel. However, the required rigidity excessively increases as α increases if a lower yield strength steel is used for the stiffeners, particularly when high-strength steel is used for the girders.

It should be noted that the effect of the elastic support by the web on the T-section is not considered in Eq. (6). Supplemental researches, including nonlinear numerical analysis and possible experiments, are necessary for Eq. (6).

7. Conclusions

The buckling strengths of stiffened webs with flat plate-shaped single-sided longitudinal stiffeners were numerically investigated in relation to the requirements for the rigidity of longitudinal stiffeners. Major findings can be summarized as follows.

The numerical analysis confirmed that the optimum location of the longitudinal stiffener is $0.4D_c$ in the simply supported web model and $0.45D_c$ in the clamped web model, where D_c is the web depth in compression in the elastic range. Practical design values for the optimum location are identified around $0.42D_c$ due to the effects of constraining the web rotation by the compression flanges.

AASHTO LRFD specifications (2014) predict buckling strengths to be on the conservative side in most cases. However, the buckling strengths from AASHTO can be slightly overestimated, resulting in a critical or a slightly unsafe design when the stiffener location (d_s) is at less than $0.4D_c$. To derive a modified lower bound for the buckling coefficients, a new design equation, i.e., Eq. (9) has been proposed based on multi-variable regression analyses incorporating both the stiffener location and the stress ratio.

The required rigidity of the equivalent T-section, which is consisted of the longitudinal stiffener and a portion of the web, was reviewed to ensure the proposed buckling coefficients and to form appropriate nodal lines. It was found that the AASHTO LRFD specifications provide the required rigidity of the stiffener on a rather unconservative side when the aspect ratios of the web panel are less than 1.0, while it yields reasonable or conservative side in the range of aspect ratios greater than 1.0. In order to overcome this limitation, a new lower bound for the rigidity requirement for longitudinal stiffener was proposed in Eq. (11).

Finally, it was suggested that a supplementary research for the required radius of gyration of the T-section given in Eq. (6) should be carried out, which is stipulated in the AASHTO LRFD specifications as a regulation to prevent the lateral buckling of the T-section.

Acknowledgments

This research was supported by a grant (13SCIPA01) from the Smart Civil Infrastructure Research Program funded by Ministry of Land, Infrastructure and Transport (MOLIT) of the Government of Korea and the Korea Agency for Infrastructure Technology Advancement (KAIA).

References

AASHTO (2014), *LRFD Bridge Design Specifications*, 7th Edition, American Association of State Highway and Transportation Officials, Washington, U.S.A.

ABAQUS (2014), *Analysis User's Manual, v6.14*, Dassault Systems, U.S.A.

Alinia, M.M. and Moosavi, S.H. (2008), "A parametric study on the longitudinal stiffener of web panels", *Thin-Wall. Struct.*, **46**(11), 1213-1223.

Allison, P.D. (1999), *Multiple Regression: A Primer*, Sage Publications Ltd., London, U.K.

Azhari, M. and Bradford, M.A. (1993), "Local buckling of I-section beams with longitudinal web stiffeners", *Thin-Wall. Struct.*, **15**(1), 1-13.

Basler, K. and Thürlimann, B. (1961), "Strength of plate girders in bending", *J. Struct. Div.*, **87**(ST6), 153-181.

Bleich, F. (1952), *Buckling Strength of Metal Structures*, McGraw-Hill.

CEN (2006), *Eurocode 3: Design of Steel Structures-Part 1-5: Plated Structural elements*, EN 1993-1-5, European Committee for Standardization, Brussels, Belgium.

Cho, E.Y. and Shin, D.K. (2011), "Elastic web bend-buckling analysis of longitudinally stiffened I-section girders", *J. Steel Str.*, **11**(3), 297-313.

Choi, B.H., Hwang, M., Yoon, T. and Yoo, C.H. (2009), "Experimental study of inelastic buckling strength and stiffness requirements for longitudinally stiffened panels", *Eng. Struct.*, **31**, 1141-1153.

Cooper, P.B. (1967), "Strength of longitudinally stiffened plate girders", *J. Struct. Div.*, **93**(ST2), 419-451.

Dubas, C. (1948), "Contribution to the study of buckling of stiffened plate", *Proceedings of the 3rd Conference on Int. Assoc. Bridge and Struct. Eng.*, 129.

Frank, K. and Helwig, T.A. (1995), "Buckling of webs in unsymmetric plate girders", *Eng. J.*, **Second Quarter**, 43-53.

Issa-El-Khoury, G., Linzell, D.G. and Geschwindner, L.F. (2014), "Computational studies of horizontally curved, longitudinally stiffened, plate girder webs in flexure", *J. Constr. Steel Res.*, **93**, 97-106.

Kim, K. (2013), "Local buckling behaviors of flat-type stiffeners in stiffened plate system", *J. Kor. Academ.-Industr. Cooperat. Soc.*, **14**(12), 6521-6526.
Maiorana, E., Pellegrino, C. and Modena, C. (2011), "Influence of longitudinal stiffeners on elastic stability of girder webs", *J. Constr. Steel Res.*, **67**(1), 51-64.
Massonnet, C. (1954), *Essais De Voilement Sur Poutres à Âme Raidle*, Publications, Int. Assoc. Bridge and Struct. Eng., Zurich, Switzerland, **14**, 125.
Park, Y.M., Lee, K.J., Choi, B.H. and Cho, K.I. (2016), "Modified slenderness limits for bending resistance of longitudinally stiffened plate girders", *J. Constr. Steel Res.*, **122**, 354-366.
Rockey, K.C. (1958), "Web buckling and the design of web-plates", *Struct. Eng.*, **36**(2), 45-60.
Rockey, K.C. and Leggett, D.M.A. (1962), "The buckling of a plate girder web under pure bending when reinforced by a single longitudinal stiffener", *Proc. Inst. Civil Eng.*, **21**, 161-188.
Shin, D.K., Cho, E.Y. and Kim, K. (2013), "Ultimate flexural strengths of plate girders subjected to web local buckling", *J. Steel Str.*, **13**(2), 291-303.
Timoshenko, S.P. and Gere, J.M. (1963), *Theory of Elastic Stability*, McGraw-Hill.
Ziemian, R.D. (2010), *Guide to Stability Design Criteria for Metal Structures*, 6th Edition, John Wiley & Sons.

Notations

A_{fc}	area of the compression flange
A_{ft}	area of the tension flange
A_s	area of the longitudinal stiffener
b_s	projecting width of the longitudinal stiffener
D	web depth
D_c	depth of the web in compression in the elastic range
D_{plate}	bending rigidity of the web plate
d_o	spacing of the transverse stiffeners
d_s	distance between the longitudinal stiffener and the inner surface of the compression flange
E	elastic modulus of steel
F_c	compressive stress on the top of the web
F_{crw}	nominal web bend-buckling resistance
F_t	tensile stress on the bottom of the web
F_{yc}	yield strength of the compression flange
F_{ys}	yield strength of the longitudinal stiffener
I_l	moment of inertia of the T-section with respect to its neutral axis
k	elastic web bend-buckling coefficient
r_s	radius of gyration of the T-section with respect to its neutral axis
R_h	hybrid factor
t_s	thickness of the longitudinal stiffener
t_w	web thickness
a	aspect ratio of the web
γ	rigidity ratio of the stiffener to the web plate
δ	cross sectional area ratio of the longitudinal stiffener to the web plate
ν	Poisson's ratio of steel
ψ	stress ratio in the web